IJST EXPLORE International Journal of Science and Technology
CENTRE OF PROFESSIONAL RESEARCH PUBLICATIONS
ISSN 2049-7318

International Journal of Science and Technology Volume 3 No. 10, October, 2014

Transport of Arsenate with Iron Hydroxide Nanoparticles in Saturated Sand: Effects of Solution Ionic Strength, pH, and Humic Acid

Mpinda T. Martin[1, 2], Abass K. Olusegun[1, 2*]

[1] Department of Environmental Science and Engineering, School of Environmental Studies, China University of Geosciences, Wuhan, 430074, P. R. China

[2] State Key Laboratory of Biogeology and Environmental Geology, China University of Geosciences, Wuhan, 430074, P. R. China

ABSTRACT

This study aims to understand the co-transport of $Fe(OH)_3$ nanoparticles and arsenate in saturated sand column and the associated influence of pH, humic acid and ionic strength on the transport. HYDRUS-1D computer program was used to simulate the sorption and transport of $Fe(OH)_3$ nanoparticles with arsenate through calibration of the breakthrough curves (BTCS). Data from different dissimilar (pH, Humic acid, and Ionic strength) input concentrations were compared to identify their influences on the nanoparticles and arsenate transport and sorption.

Results from this study indicated that transport of iron hydroxide nanoparticles was influenced not only by ionic strength, humic acid, ionic composition and pH, but also by the flow velocity, nature and size of suspended nanoparticles. Nanoparticles were very mobile at low ionic strength, while increasing salt concentration decreased mobility, and consequently the amount of particles retained in the column increased. The transport of iron hydroxide nanoparticles became normalized due to the availability of (OH^-) at pH 7-9. Below this pH value, the iron hydroxide nanoparticles precipitates, increasing the amount of (OH^+) than (OH^-) on the surface of the adsorbent.

Conversely, the transport of arsenate was reduced under strongly acidic and alkaline conditions. Humic acid had considerable influence on the mobility of arsenate, resulting in more adsorption and less transport. A major implication of this study was that changes in chemical composition of solutions in aquifers and vadose zones might result in a different transport mechanism for nanoparticles as well as the associated transport of adsorbed arsenic.

Keywords: *Arsenate, Iron hydroxide, Co-transport, Adsorption*

1. INTRODUCTION

Nanoparticles are ubiquitous in the environment and may influence environmental water quality. They may facilitate the transport of otherwise immobile contaminants such as highly hydrophobic substances (Hasselov et al., 2008; Mueller et al., 2008; Hochella et al., 2008; Hofmann et al., 2007; Yang et al., 2010). The fate and transport of nanoparticles in the environment are controlled by many physical and chemical variables, such as solution ionic strength, pH, and surface charge. Compared to colloids or other emerging contaminants, nanoparticles pose new challenges for scientists. Engineered and naturally occurring nanoparticles can be found in various shapes, for example, carbon nanotubes have a high aspect ratio (Lecoanet et al., 2004). It is already obvious that particle size and environmental conditions plays an important role in the transport and deposition of both colloids and nanoparticles. Wang et al. (2012) and Lecoanet et al. (2004) observed that the role particle shape plays on nanoparticles transport in the environment is less understood.

In the soil environment, the dominant forms of arsenic are arsenate [As (V)] under aerobic conditions and arsenite [As

(III)] under anaerobic conditions. Iron hydroxides [$Fe(OH)_3$] in particular have high affinity to As (V) and form inner-sphere surface complex via a ligand exchange mechanism (Waychunas et al., 1993). It has often been found that a significant portion of the mobile arsenic is present in the nanoparticles form, i.e., arsenic minerals or adsorbed arsenic on mineral surfaces. Mobilization and transport of nanoparticles were found to be highly dependent on several factors especially ionic strength, pH, and organic matter. Literature results indicate that a significant amount of colloidal particles would be mobilized when the background solution (0.01 M NaCl) is displaced with deionized water. This was based on the high level of turbidity (>100 NTU) in the effluent solution (Roco, 2005; Helland et al., 2006; Siegrist et al., 2007).

According to clean-bead filtration theory (CFT) (Yao et al., 1971 and Megan, 2012), particle transport and deposition in porous media can be described as a two-step process, i.e., transport and adsorption. Step one explains the transport of nanoparticles to the vicinity of grain (collector) surface, govern by three mechanisms including interception, gravitational sedimentation, and diffusion. Transport is typically quantified by the single collector efficiency (η) which reflects the frequency of particle collisions with the grain surface (Tufenkji et al., 2004; Megan, 2012). The second step, involves attachment to the grain (collector) surface which is directly related to the interaction energy between the particle and the collector surfaces. The attachment is typically quantified by the collision efficiency factor α, which represents the fraction of the collisions that lead to successful attachment. Currently, no single theory can predict α when the surface charges of the particles and collector are opposite, namely under unfavourable conditions.

Mobilization and transport of nanoparticles were found to be highly dependent on several factors especially ionic strength (Zhang, 2006). The changing ionic strength will mobilize colloid particles (e.g., iron and aluminium oxides and hydroxides) which has high absorption capacity for arsenic, leading to nanoparticles facilitated transport of highly toxic arsenic. In general, the results of particle transport experiments often do not agree with the qualitative predictions based on the theory (Elimelech et al. 1995). Many studies have been conducted to understand the transport of colloid and nano-sized particle transport in porous media (Wang et al., 2012; Lecoanet et al, 2004; Ben-Moshe et al., 2010; Megan, 2012).

Arsenic is a serious problem affecting groundwater contamination. Many studies have focused on understanding the effects of arsenic (As) in groundwater but there still remains a knowledge gap on the process optimization and the co-transport of As in the presence of iron hydroxide, effects of pH, HA, and ionic strength (IS) on As in the presence of iron hydroxide during transport. This could have a tremendous effect on As remedial effort in groundwater contamination event. Hence, in this study, we focus on the design of a functional model that will help to resolve problems associated with arsenic contamination in groundwater, of particular interest, is the process involving the transport mechanism of arsenate contaminants in groundwater. This knowledge will aid better decision when choosing an effective remedial means for site-specific groundwater contamination and chemistry. Besides, many works have been conducted in the area of arsenic redox transformation in groundwater but little or none explained the effect of iron hydroxide nanoparticles on arsenate co-transport in saturated aquifers. However, few studies investigated the mobility of arsenate under dynamic flow conditions. Thus, this research work will contribute to the understanding of factors influencing transport and adsorption in relation to changes in ionic strength, pH value, and humic acid.

2. MATERIALS AND METHODS

2.1 Reagents and Analytical Method

Stock solutions of 100µg/l arsenate were prepared from a 1mg/l stock solution (Commercial standard solutions, National Standard Material Centre of China) were used. Working standard solutions of arsenate were prepared by stepwise dilution of the stock solutions just before use. All reagents were of analytical-reagent grade and water purified with a Milli-Q system (Millipore) was used throughout the experiment. Total arsenic concentrations were measured using Hydride Generation-Atomic Fluorescence Spectrophotometer (HG-AFS, Rayleigh China). Adsorption isotherms, two-site non equilibrium transport model, using software like HYDRUS-1D with equilibrium model of Vangenuchten were used to model the flow characteristics.

2.2 Quartz sand preparation

Quartz sand with median grain diameter (d_{50}) of 1~2 mm obtained from Huazhong University of Science and Technology, China was used as model granular media for column experiments. Prior to use, the sand was washed thoroughly to remove any metal oxide and attached clay on the grain surface. The sands were immersed in 0.01 M NaOH solution for 24 hours, rinsed with deionized water, and then soaked in 0.01 M HCl solution for another 24 hours before a final thorough rinsing with deionized water. The sands were then dried in an oven at 105°C.

2.3 Preparation of iron hydroxide suspensions nanoparticles

Chemical Analysis: The iron hydroxide nanoparticles were produced from iron (III) chloride, a dark brown hexagonal crystal, hygroscopic, with density of 2.898g/cm^3, highly soluble in water (74.4g / 100g water at 0℃) and organic solvent such as ethanol, ether and acetone. All solutions used were prepared using deionized (DI) water. The proportion of $FeCl_3$ used up in the reaction is expressed as:

$$FeCl_3 + 3H_2O \rightarrow Fe(OH)_3\ (\text{nanoparticles}) + 3HCl$$

Boiling distilled water was added drop-wise at 1- 2ml to saturated $FeCl_3$ solution and heated continuously until the liquid became reddish brown. Care was taken to ensure that saturated solution of $FeCl_3$ was used to prevent non-formation of ferric hydroxide nanoparticles when chloride is at low concentration. Because nanoparticles are meta-stable, reaction conditions were controlled to prevent the precipitation of $Fe(OH)_3$. On appearance of a reddish brown colouration, the heat applied is immediately removed to avoid coagulation of already formed nanoparticles.

2.4 Characterization of iron hydroxide suspensions nanoparticles

Zeta (ζ) potentials, streaming potentials and dynamic light scattering (DLS) were used for the characterization of the nanoparticles. Streaming potentials were converted to ζ-potentials using the Helmholtz-Smoluchowski equation. This ζ-potential information was applied in conjunction with the DLVO theory to calculate total interaction energies of iron hydroxide suspensions nanoparticles. Results from the analysis shows a zeta potential value of 7.5 mV and the distribution size of 20.1nm (Table 1). This value implies that the nanoparticles are in an unstable state. The grain diameter and zeta potential of $Fe(OH)_3$ suspensions and quartz sand powder were measured separately using Dynamic Light Scattering (DLS) on a Malvern instrument (DTS 3.32, MAL500399). The DLS measurements were conducted with a multi-detector light unit which utilizes a laser with a wavelength of 510nm. All characterization measurements were carried out in duplicate using freshly prepared suspensions for each condition.

$Fe(OH)_3$ concentrations in the influent and effluent were measured with UV- spectrophotometry (UV-1800PC/MAPADA) at Wavelength of 510 nm, respectively. Before every experiment, calibration curves of $Fe(OH)_3$ were constructed by diluting their original inflow suspensions into a series of standard solution at different concentration separately. As proved, Fe^{3+} concentration spectrometer response was linear with a coefficient of determination of $R^2 \geq 0.999$ between concentration ranges of 0-50 mg/l.

Table 1. Zeta potential size and distribution

Parameters		**Mean (mV)**	**% PDI**	**Width (mV)**
ZetaPotential (mV): 7.593	Peak1:	-2.854	89.05	7.703
Std. Deviation (mV): 30.81	Peak2:	92.56	10.95	9.04
Conductivity (mS/cm): 23.12	Peak3:	0	0	0
Size dist. by intensity		**Diam. (nm)**	**% Intensity**	**Width (nm)**
Z-Average size (nm): 20.1	Peak1:	9.149	100	2.036
Polydispersity index: 0.109	Peak2:	0	0	0

Peak3:	0	0	0

2.2.3 Co-transport Experiment

Saturated transport experiments were performed using glass columns (2.5cm in inner-diameter and 10.0cm in length). The vertically oriented columns were wet-packed with tested sand. Column experiments were run in an upward flow mode using a peristaltic pump (Figure 1). Before initiating a transport experiment, the packed column was preconditioned with >10 pore volumes (PVs) of DI water at a flow rate of 3 ml/min. A nonreactive tracer experiment was then performed by injecting 1.0 PV of NaBr solution into the column and then eluted with 3.0 PVs of DI water. Sodium bromide was used as a conservative nonreactive tracer to characterize the water movement in columns. Column effluents were collected using a fraction collector.

After the tracer test, two-phase transport experiments were performed. Phase 1: arsenate concentration of 100µg/l bearing iron hydroxide suspensions at a concentration of 50mg/l (C_o = inlet conc. and C = outlet conc.) in solutions of varying IS, pH and HA. Phase 2: several PVs of iron hydroxide-free background electrolyte solution with the same IS, pH and HA were pumped into the column to ensure that almost no particles were detected in the effluent. The concentrations of the nanoparticles in the effluents were measured spectrophotometrically. The breakthrough curves (BTCs) were plotted as dimensionless concentrations (C/C_o = relative concentration) of iron hydroxide suspensions (or/and As) as a function of time.

Fig. 1. Laboratory set-up showing the column experiment

3. THEORETICAL MODEL

3.1 Two-site Kinetic non-equilibrium adsorption

The two–site kinetic adsorption model described below is the same model as discussed by (Selim et al., 1976) and by (Cameron et al., 1977). The two-site model assumes that the sorption sites could be described in two fractions; adsorption on one fraction (‘‘type-1’’sites) which is assumed to be instantaneous, while adsorption on the other fraction (‘‘type-2’’ sites) which is thought to be time-dependent. At equilibrium, adsorption on both types of sorption sites are described by linear equations explained in the preceding section (Maraqa et al., 2011 and Liu et al., 2013).

3.2 Particle transport equations

The general equation describing solute transport under one-dimensional, steady-state water flow in porous media is given as:

$$\theta \frac{(\partial C)}{(\partial t)} + \frac{\rho \partial a}{\partial t} = \theta \frac{D \partial^2 C}{\partial x^2} - \theta \frac{Po \partial C}{\partial x} - \theta \lambda_l c - \rho \lambda_s a \quad [1]$$

As proposed by Maraqa et al., (2011), C is the concentration in the liquid-phase [ML^{-3}], a is concentration on the solid phase [MM^{-1}], D is the dispersion coefficient [L^2T^{-1}], P_o represents the average pore-water velocity [$L T^{-1}$], with a soil bulk density ρ, having a volumetric water content, θ. The first-order decay constant of the liquid phase and solid phase is λ_l and λ_s respectively with a dimension unit [T^{-1}]. t and x represents the time (T) and distance [L].

The breakthrough curves were simulated using the inverse solution algorithm HYDRUS-1D (Simunek et al., 2008). The governing flow and solute transport equations were solved using the Galerkin-type linear finite element method with a Grank-Nicholson time weighting scheme. Two-site sorption model (chemical non-equilibrium) was used to simulate the breakthrough curves. The concept of two site sorption (Vangenuchten and Wagenet, 1989) was implemented in HYDRUS to permit consideration of non-equilibrium adsorption-desorption reactions (Liu et al., 2013). The two-site sorption concept assumed that the sorption sites could be divided into two fractions:

$$S_k = F_{r1} + F_{r2} \quad k\epsilon\,(1, n_s)$$

[2]

Sorption, F_{r1} on one fraction of the sites (the type-1 sites) was assumed to be instantaneous, while sorption, F_{r2} on the remaining (type-2) sites was considered to be time-dependent.

$$F_{r1} = \mathrm{F}\, S_k \quad k\epsilon\,(1, n_s)$$

[3]

$$F_{r2} = (1 - F)\, S_k\, k\epsilon\,(1, n_s)$$

[4]

Where F is the fraction of sorption sites assumed to be in equilibrium with the solution phase and is given as:

$$\mathrm{F} = \frac{V1}{V1 + V2}$$

[5]

Where v1 [L^3] and v2 [L^3] are the volume of the the type-1 and type-2, respectively.

The linear equation for sorption equilibrium is:

$$S_k = K_d\, C_{e,k} \quad k\epsilon\,(1, n_s)$$

[6]

Where K_d was the partition coefficient [$L^3\ M^{-1}$], and $C_{e,\,k}$ was the k solution concentration at equilibrium.

Total adsorption $S_{k,}$ was simply:

$$S_k = F_{r1} + F_{r2} \quad k \in (1, n_s)$$

[7]

Thus at equilibrium the total sorption on the two sites was given as:

$$S_k = FK_dC_{e,k} + (1 - F)K_d\, C_{e,k} \quad k\epsilon\,(1, n_s)$$

[8]

Because type1 sites were always at equilibrium, it followed from Eq.3 that:

$$\frac{\partial F_{r1}}{\partial t} = FK_d \frac{\partial C_{ek}}{\partial t} \quad K \in (1, n_s)$$

[9]

The rate of mass transfer to and from the type-2 non-equilibrium sites was modelled as first order. Under the first–order mass transfer approach, sorption on the type-2 non-equilibrium sites was given as:

$$\frac{(\partial F_{r2})}{(\partial t)} = \alpha[(1 - F)K_d\, C_{e,k} - F_{r2}] \quad k\epsilon\,(1, n_s)$$

[10]

Where α was the first-order sorption rate coefficient [T^{-1}]. The unknown parameters for the models were estimated either by fitting model predictions to experimental breakthrough curves, or by independent measurements.

4. RESULTS AND DISCUSSION

4.1 Transport model of pH effect on $Fe(OH)_3$ nanoparticles

One of the soil characteristic in this present work, i.e., the bulk density (ρ), was measured from the column

characteristics and was estimated at 1.46gcm^{-3}. The volumetric water content (θ) and the velocity were calculated at 0.43 and 20.46659 m/day respectively. These parameters were applied for better understanding of the processes that occurred during the transport. Parameters D, F, K_d and α were determined by inverse estimation using the Marquardt-Levenberg optimization algorithm included in HYDRUS-D.

For a two-site non-equilibrium model, R was the retardation coefficient and is defined as:

$$R = 1 + \frac{\rho K_d}{\theta}$$

[11]

K_d is the partition coefficient/absorption and F is the fraction at sorption sites. 1/R value is the ratio of the transport velocities of contaminants and water. Simulation parameters derived from the fitting of data for the study of the impact of pH on the transport model is shown in Table 2. Trend parameters of $Fe(OH)_3$ nanoparticles showing the effect of pH revealed that the parameters α and K_d decreased between pH 5 and 10; and when in association with As (V), while the parameters D and F increased.

Table 2 Results of fitting adsorption and transport models

Solution	A	K_d	D	F
Blank test	0.01	0.01	0.3	0.01
pH7+$Fe(OH)_3$	0.03	0.01	0.3	0.7
pH10+$Fe(OH)_3$	0.04	0.7	0.2	0.08
IS[0.001]+$Fe(OH)_3$	0.01	0.5	0.3	0.6
IS[0.01]+$Fe(OH)_3$	0.01	0.5	0.2	0.1
IS[0.1]+$Fe(OH)_3$	0.01	0.01	0.4	0.2
HA + $Fe(OH)_3$	0.3	0.9	0.4	0.3
As(V)+pH10	0.01	0.01	0.2	0.3
As(V)+IS [0.01]	0.7	0.1	0.4	0.5
As(V)+$Fe(OH)_3$	0.01	0.6	0.1	0.4
AS(V)+HA	0.01	0.1	0.2	0.2
pH 5	0.2	0.01	0.2	0.9

In general, the fraction of sorption for Type 1 (F_{r1} or F) which usually occurred within the surface molecule decreased from 0.9 to 0.08 when going from pH 5 to pH 10, while K_d increased from 0.01 to 0.5 for the same range of pH. The dispersivity D, increased from the value 0.2 to 0.3 while α decreased in value from 0.2 to 0.04, this could be either as a result of increase in pH from 5 to 10 or the sand characteristics and interacting molecules involved during the transport. At the same time, α decreased from the value 0.9 to 0.08. This was likely due to surface charge heterogeneity on the quartz grains, i.e., metal oxide patches, surface roughness of the sand grains, and enhanced nanoparticles retention in low velocity regions. Li et al., (2008), also suggested the existence of metal (Hydroxides) oxide patches on thoroughly cleaned quartz grains.

Type 2 fraction, F_{r2} usually takes place due to penetration of the microspores in solution during transport and are often absorbed by the walls of the molecules. At the end of the experiment, the value of F_{r2} was increased by 82%, when the pH allowed a fast penetration at the structural portion. However, the fraction of type 1 decreased from 0.9 to 0.08, at the initial to the final run of the experiment respectively. At the same time, the first order sorption rate coefficient for one-site or two-site non equilibrium adsorption, α, decreased from 0.2 to 0.04 while there is substantial reduction of F_{r1} in case of As (V) + pH10 compared with pH 5 during the transport of $Fe(OH)_3$ nanoparticles. The decrease in α value was also visible in the case of nanoparticles transport with arsenate at pH 10, which was

0.01 compared to pH 5, which was 0.2. Low value of α means, the solute were slowly transferred to type-2 sites while in a reverse situation, high value of α value means the solute was easily transferred into type-2 sites. In a study conducted by Carabante, (2012), he observed the influence of pH on the adsorption of arsenate in the presence of iron oxide. Furthermore, it was observed that the adsorption of arsenate on iron oxides involved interactions between the adsorbate and the hydroxyl group of iron hydroxide (oxide) which consequently had a profound effect on the transport of the nanoparticles.

The partitioning coefficient between the solid and aqueous phases (Kd), at different pH values range, varied from 0.28 – 0.3 indicating an increase in mass transfer between contaminant phases. Hence, the pH had a significant influence on the solute diffusion into the soil particles. Additionally it showed that the surface chemistry of iron hydroxide (oxides) varied with pH.

4.2 Experimental Influence of pH on $Fe(OH)_3$ transport

The influence of pH on iron hydroxide transport is shown in Fig. 2. Here, we observed that the column saturated faster when the pH value was set at 7. Three apparent trends were identified within the first 10mins and the flow was uniform. At t = 18 minutes, significant increase in concentration of the nanoparticles were observed. During this build-up, two of these trends emerged, the first, was initiated at pH 7 which reached its saturation point at a relative concentration of 0.7 and stabilizes around 0.65. Adjusting the pH of the solution from 10 to 7 drastically reduced the peak-concentrations and mass recoveries and thus enhancing the transport of the nanoparticles. However, at pH 5, 10 and pH 10 associated with As(V), the nanoparticles saturation was delayed relative to the maximum relative concentration and a long stabilization period was observed, which extends between the time t = 20 mins and 100mins, before desorption set in.

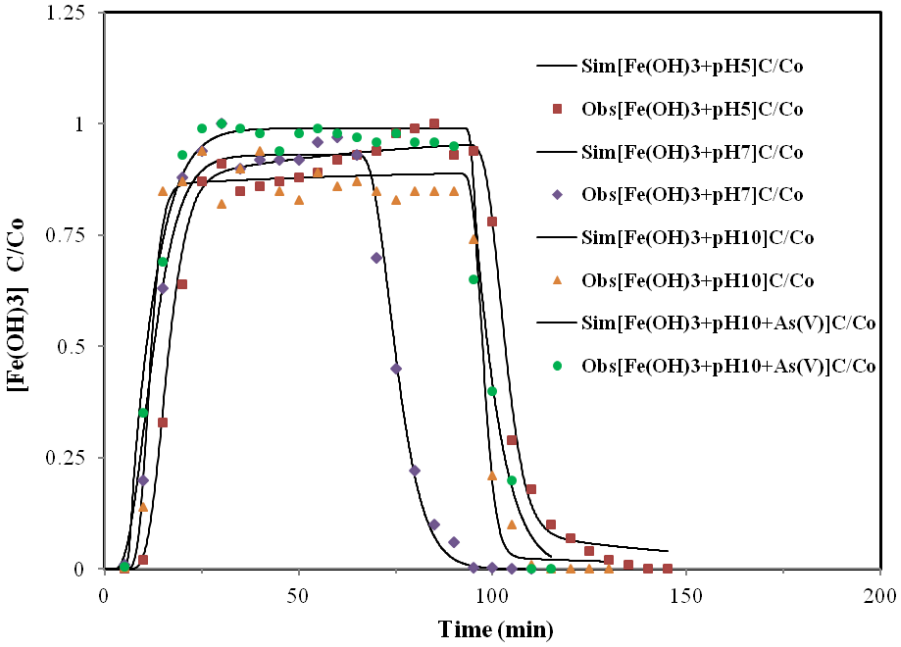

Fig 2. Effect of pH on $Fe(OH)_3$ (Flow rate = 3ml/min, [IS]= 0.01mol/L, $[As^{5+}]$ = 0.1mg/L, [Fe] = 50mg/L)

At low pH, the hydroxyl groups, at the surface of the iron hydroxide (oxide) are doubly protonated ($FeOH^{2+}$) and the surface charge of the iron hydroxide (oxide) is thus positive. A maximum adsorption of arsenate had been observed at acidic pH values around 5. At these pH values, the electrostatic attraction between the negative oxoanion and the positive charge of the iron oxide surface favoured adsorption. At pH lower than 3, fully protonated arsenate (H_3ASO_4) species were present in solution and electrostatic attraction was no longer possible, resulting in a lower adsorption.

In this study, for strongly acidic conditions with pH 3-5, the iron hydroxyl precipitated, causing an increase in the concentration of H^+ which became higher than the OH- into the solute in contact with the sandy column. Consequently the transport and adsorption reduced due to the non penetration of the precipitated solute molecules in the sandy particle pores and their absence on the particle surface.

Adsorption increased dramatically as the pH decreased, and extreme acidity (pH=3) inhibited the adsorption and the transport. Smedley et al., (2001), obtained similar results. They studied As (III) and As (V) mobility with groundwater's using radioactive As ($t_{1/2}$=17.7days) and As ($t_{1/2}$=26.4 hours) to monitor the breakthrough of As. They found that; As(III) moved 5-6 times faster than As(V) under oxidizing conditions (pH 5.7); with a neutral groundwater (pH 6.9), As(V) moved much faster than under (i) but was still slower than As(III); under reducing groundwater (pH 8.3), both As(III) and As(V) moved rapidly through the column; and when the amount of As injected was substantially reduced, the mobility of the As(III) and As(V) was greatly reduced. As earlier explained, similar observation were made in this study. The transport of As was reduced, and at certain pH values, the transport couldn't occur. For the pH range values of 7 to 9, the transport became normal due to the availability of (OH^-), which enhances the transport. Below this pH value, the iron hydroxide may precipitate, increasing the amount of (OH^+) than (OH^-) on the surface of the adsorption. This phenomenon slowed the speed of the solute at the same time, the transport.

4.3 Influence of the ionic strength on $Fe(OH)_3$ nanoparticles transport

The results of the influence of the ionic strength on $Fe(OH)_3$ nanoparticles transport are shown in figure 3. We observed that the column saturated faster when the ionic strength concentration was 0.01mol/.

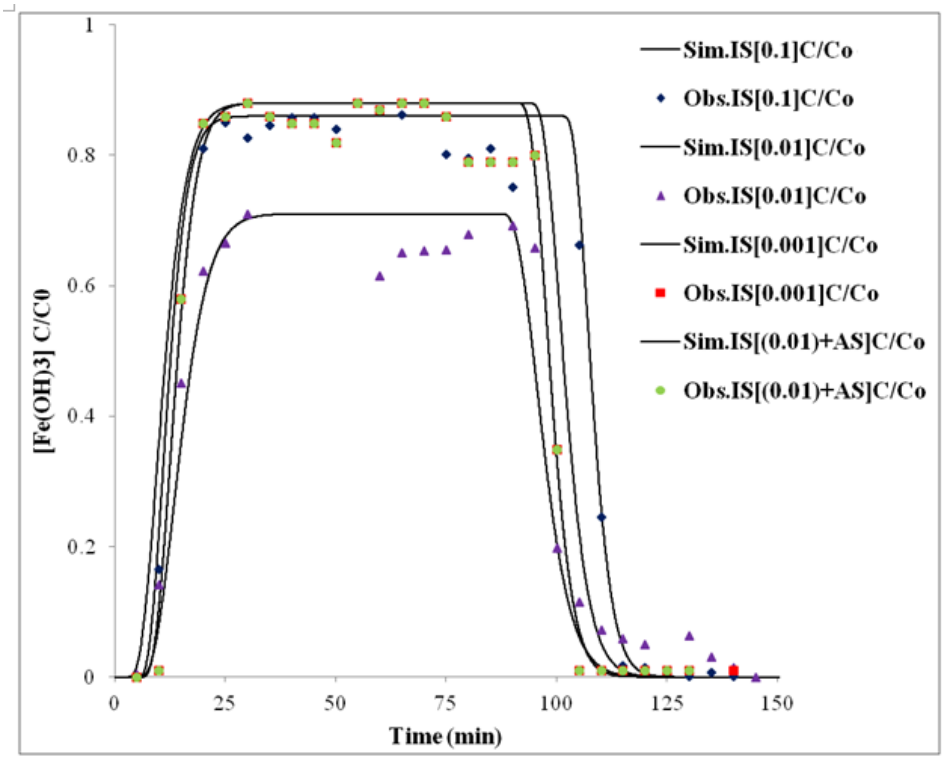

Fig 3. Effect of ionic strength on $Fe(OH)_3$ (pH = 6.9, Flow rate=3ml/min, [As] = 0.1mg/L , [Fe] = 50mg/L)

From the figure, there was a rapid deviation of ionic strength concentration and transport of $Fe(OH)_3$ was achieved quickly at time t = 10 and t = 15 minutes. Particle mobility was greatly influenced by the salt concentration under typical salt content in groundwater. An increase in the ionic strength from 0.001M to 0.1M resulted in decrease of the adsorption isotherm coefficient (K_d) and fraction of sorption F_{r1} and increase in the dispersion (D) value. However, α, remain constant. The IS at 0.01 associated with arsenic yielded a noticeable increase in the parameters α, D and F, while K decreased, resulting in an increase in the mobility of the $Fe(OH)_3$ nanoparticles associate with arsenate. Furthermore, the high transport rate could be as result of exchange in ionic capacity: the high ionic strength tends to eliminate the effect of the weak ionic charges, replacing the surface charge, and leaving less space to other types of ions. Increase in salt concentration increase the adsorption and reduces the transport. Similar results were found in the study conducted by (Liping et al., 2001). They reported that transport of contaminants in groundwater systems could be affected by physical non-equilibrium

processes (e.g., caused by aquifer heterogeneity, preferential flow, and kinetic diffusion) or/and chemical non-equilibrium processes (e.g., caused by kinetic sorption/ion exchange and hysteresis sorption).

As a general rule, ferryhydrite particles were very mobile at low ionic strength, while increasing salt concentration decrease mobility, and consequently the amount of particles retained in the column increased. During the deposition step, comparing tests performed at different ionic strengths showed that increasing ionic strength resulted in retardation breakthrough curve and thus to an increase attachment rate. Same results were obtained by (Tosco et al., 2012).

Fuller et al., (2003) and Puls et al., (1992), conducted column experiments with aquifer material to investigate possible effects of iron hydroxides nanoparticles on facilitating As (V) transport. They observed the mobilization of nanoparticles-associated arsenate when flushing the column with DI water. Moreover, they evaluated several factors (particle size, pH, velocity, ionic strength, and anions) on the transport of Iron hydroxides nanoparticles. Their results demonstrated that the presence of $HAsO_4$ increased the mobility of iron hydroxides due to increased particle- particle repulsive forces.

From our experiment, the ionic strength value was seen to have an effect on the percentage of arsenic removed. However, the effect of ionic strength was more pronounced at higher pH. The solution ionic strength (IS) and ionic composition (IC) are known to have a large influence on the transport behaviour of colloid-associated contaminants.

4.4 Influence of Humic acid on Fe $(OH)_3$ nanoparticles transport

Results showing the influence of humic acid are displayed on figure 4. It can be observed from the figure that the column saturated faster when humic acid was coupled with arsenate and sparsely delayed in the case of humic acid with iron hydroxide only.

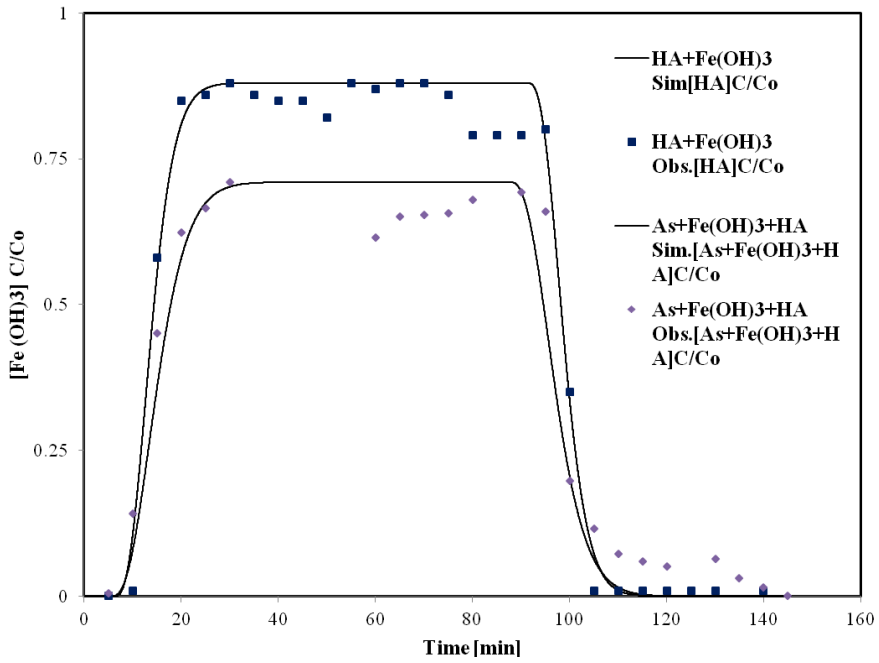

Fig 4. Effect of Humic acid on Fe $(OH)_3$ (pH=6.9, Flow rate=3ml/min, [HA] = 20mgL^{-1}, [As] = 0.1mg/L, [Fe] = 50mg/L)

Transport here occurred at around 10min during the initial stage. The shape of the curve was such that the two curves gave almost the same characteristics. With regards to humic acid in combination with arsenate, saturation was a little faster, but the difference was barely noticeable, however it had approximately similar values. The transport was more effective between t = 10min and t = 100min. At t =100min, the descent was gradual until the final time was reached at t = 110 min. Simulation parameters derived from the fitting data used for the study of the impact of HA can be found in table 2. In general, the trends for the transport of $Fe(OH)_3$ and As (V) were characterized by a build-up in value in the case of parameters D, F, K_d and alpha, during the interaction of HA + $Fe(OH)_3$; although a reduction of these

parameters was observed for the AS (V) + HA experiment. This result clearly shows the impact of humic acid on the displacement of As (V). Here, arsenate was limitedly displaced.

The effects of HA and HA associated with arsenate on $Fe(OH)_3$ nanoparticles transport, was estimated using the fraction of sorption type 1 (F_{r1}), the dispersivity, the partition coefficient (K_d). We observed a decreased in these parameters while the first order sorption rate coefficient (α) increased. K_d decreased from 0.2 to 0.1, at the same time, α increased from 0.01 to 0.3, while F_{r1} decreased from 0.2 to 0.1, implying that the fraction of sites, type 2 was 80%, at the beginning of the experiment. However, at the end of the transport, HA associated with iron hydroxide gave the following; F_{r1} = 0.1 and F_{r2} = 0.9. In the case of HA with arsenate, F_{r1} values showed that about 20% of the pollutants were adsorbed on the type1 sites, while 80% were adsorbed on the type 2 sites (F_{r2}) in the first experiment (HA with iron hydroxide). This result suggested that the penetration at the beginning of the adsorption was instantaneous and superficial which occupied 10% of the surface of macro-pores, but the adsorption was only on the surface, but with time, the penetration increased to micropores leading to more adsorption. At the end of the transport, there was nearly 90% penetration observed in the micro-pores inner surface. This could be justified by the fact that, the fraction of humic acid (HA), modified the structure of the $Fe(OH)_3$ nanoparticles and arsenate, furthermore, other products could have been in contact with the soil or sediment. HA also had a great influence on the diffusion of the nanoparticles and arsenate in the sediment (sand). In natural systems, organic matter such as humic acid (HA), may have interacted with mineral oxides substances present in groundwater. This mutual interaction may affect in turn, the interfacial, as well as, the colloidal properties of the mineral, such as the surface charge, the dispersion stability, and the adsorption capacity relative to other species present in solution.

These results are similar with results reported by Kappler et al., (2003), which showed that, in addition to their function as electron shuttles, humic acids could stimulate microbial iron (III) reduction by complexation of Fe (III) or Fe (II). The first process would render Fe (III) more accessible to microorganisms, whereas the second would prevent adsorption of Fe (II) to the surfaces of the minerals and microbial cells, thus providing sufficient ‘‘free surface’’ for reduction that increases with Fe (II) concentrations. However, the actual extent of these complexing mechanisms caused by humic acids during iron reduction in natural environment still has to be determined. Wang et al., (2012), observed that the transport of $Fe(OH)_3$ and As (V), in the presence of HA, generally increased with increasing HA concentration. In a similar study, (Wang et al., 2013), showed that the transport of $Fe(OH)_3$ nanoparticles increased with increasing HA concentration, largely because of enhanced repulsive interaction energy between nanoparticles.

Wei et al., (2010), elucidate that the presence of humic acid (HA) in water poses environmental problems because it enhanced the transport of several contaminants. A series of column experiments was conduct in this work toward studying HA transport in different porous media under various pH, ionic strength, and flow rate conditions. The results showed that decreasing pH and increasing ionic strength, increases adsorption and therefore delayed the transport of humic acid in porous media. However, increasing flow rate accelerated the transport of HA in porous media. The effects of pH, ionic strength, and flow rate varied with the solid matrix and were more evident in sands of smaller average particle diameter than in those with larger ones. These results also suggest that HA adsorption was an important process controlling HA transport and should be considered in studies of HA behaviour in porous media. The column saturated soon when humic acid was reacted with iron hydroxide and was achieved at a faster rate when humic acid was associated with arsenate. It is well known that HA is a natural organic polyelectrolyte having anionic functional groups, such as carboxylic and phenolic groups. These functional groups may have strong interactions and/or form complexes, with trace metal ions.

4.5 Influence of pH, ionic strength and humic acid on arsenate transport

From the fitted and observed arsenate transport parameters, results of obtained for arsenate transport are shown in (Table 3). It can be observed that the column saturated faster when arsenate was in association with humic acid.

Table 3 Result of fitting adsorption and transport models for arsenate

As (V) Exp.	D	Fraction(F)	Kd	Alpha(α)
As+Fe(OH)$_3$	0.01	0.6	0.27	0.3
As+IS+ Fe(OH)3	0.01	0.6	0.20	0.2
AS+pH10+ Fe(OH)3	0.01	0.01	0.24	0.3
As+HA+ Fe(OH)3	0.26	0.1	0.21	0.1

In terms of ionic strength during As (V) transport, D and α decreased when K_d and F_{r1} increased, while considering the co-transport with the $Fe(OH)_3$ nanoparticles, it was characterized by an increase in D and F_{r1}, while α and K_d decreased, for the same experiments. Transport of As (V), with regards to the effect of humic acid was characterized by an increase in D, K_d and α when F_{r1} descended. Similarly, during co-transport with $Fe(OH)_3$ nanoparticles, D and F_{r1} increases when K_d and α decreased. Considering the effects of As (V) with $Fe(OH)_3$ during co-transport, we noticed that D and K_d decreased when alpha and F_{r1} increased in association with As (V), while D and K_d increased when α and F_{r1} decreases, during co-transport with the $Fe(OH)_3$ nanoparticles. The column transport experiments indicated strong As (V) retardation followed by slow release or extensive tailing in the breakthrough curves (Fig. 5). Sharp decrease in As (V) concentration during flow, further verified the extensive non-equilibrium condition, which was likely due to the dominance of kinetic retention (sorption-release) processes. During the transport of As (V) there was a noticeable decrease of F_{r1} from 0.2 to 0.01. This decrease was observed when the pH was adjusted to 10. The fraction of the sorption site, F at the beginning of the experiment was 10% in the macropores (F_{r1}), and 90% in the micropores (F_{r2}), while at the end of the experiment, F_{r1} was 1% in the macropores and F_{r2} was 99% in the micropores. This means that there was a greater adsorption of the pollutant in the micropores (sites type2). The regression of the adsorption coefficient (K_d) decreased from 0.6 to 0.27, which has a considerable negative impact on pollutant transport.

In general the ionic strength had a stronger influence on the transport of arsenate. K_d varied between 0.1 and 0.2, at the same time, F varied between 0.5 and 0.6. This implied that at the beginning of the experimental run, 50% of pollutants were adsorbed in the macropores and 50% were adsorbed at the surface of the micropores. At the end of the run, 60% of the pollutants were adsorbed on the macropores, 40% were adsorbed on the micropores. The results explicitly showed that the transport of arsenate under the influence of ionic strength was more favourable. Using a lower value of ionic strength slightly increased the percentage of arsenic removed, at all pH values and at all iron doses. Effluent results demonstrated that nanoparticles-facilitated transport contributed little to arsenic movement when the solution ionic strength was maintained constant. Mobilization of nanoparticles amorphous material and enhanced transport of As (V) were observed by previous authors as a result of changes in ionic strength of the input solution (Fuller et al., 2003). Puls et al., (1992), demonstrated that the presence of $HAsO_4$ increased the mobility of iron hydroxides due to increased particle- particle repulsive forces.

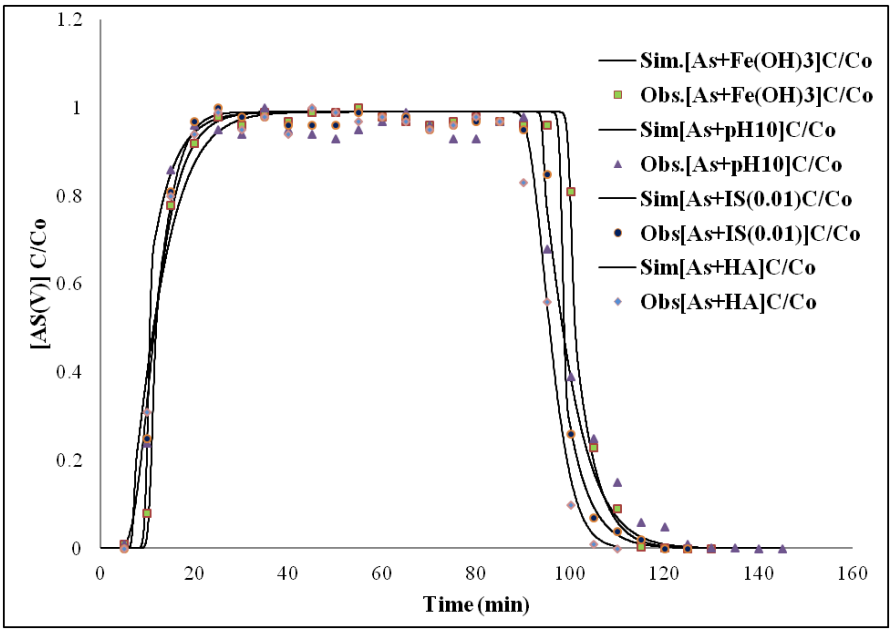

Fig 5. Effect of pH, HA and IS on As (V) (Flow rate = 3ml/min , pH=6.9, [IS]= 0.01mol L^{-1}, [As] = 0.1mg/l, [Fe] = 50mg/L).

The transport of the arsenate was influenced by the action of the humic acid. The K_d parameter for this case varies between 0.1 and 0.21 while the parameter F could vary from 0.2 to 0.1; meaning that 20% of the pollutants was adsorbed in the macropores at the beginning, while 80% was adsorbed in the micropores at the end of the run. There is a significant regression of half the initial value for F, when at the same time there is an increase of half the initial value for the K_d factor. This result demonstrates once again that the humic acid has a remarkable influence on the transport of arsenate. In this study, transport is reduced by the influence of humic acid in the presence of arsenate. Humic acid have considerable influence on the arsenic mobility; resulting in more adsorption and less transport.

The influence of pH 10 on the transport of arsenate in this study was demonstrated by varying the parameters K_d from 0.01 to 0.24 and F from 0.3 to 0.01, a significant value for the transport of arsenate, was obtained revealing that 30% of the pollutant was adsorbed in the macropores at the beginning of the run and 70% in the micropores, while 1% was adsorbed in the macropores and 90% in the micropores at the end of the experiment. The variation of the pH during this mobilization may totally change the displacement of the arsenate associate with iron hydroxide. The transport of arsenate in association with iron hydroxide in a neutral groundwater (pH 6.9-7), was much faster than under pH10. This may be the cause for the reduction in transport of arsenate in alkaline conditions. According to Carabante, (2012), at pH values above the point of zero charge, the iron oxide is negatively charged, and repels the negatively charged arsenate. Consequently, adsorption becomes substantially lower at these pH-values.

4.6 The retardation coefficient (R)

In case of a linear adsorption isotherm, the relationship between adsorption and the transport was straight forward and the partition coefficient, K_d, defined a constant for the retardation coefficient. With non-linear adsorption, which was most likely to be the case for arsenic adsorption, the value of K_d varied with concentration and was related to the slope of high concentrations and ultimately to self-sharpening and diffuse fronts. The greater the non-linearity, the longer it would take to flush completely all the arsenic from an aquifer.

From the results presented in Table 4, in general R varied from 1.33 to 2.35 for all the experiments conducted in this study. This value was very low compared to other experiments reported. 1/R factor varied from 0.4 to 0.75. β varied from 0.24 to 2.97. This result was dependent on transport speed, given that speed was important, the coefficient of retardation decreased reasonably. In a reverse condition, the speed of transport would reduce the coefficient of retardation, and resulted in higher values of R. But, for the entire experiment, the trend was the same for the three main parameters in the analyses. This notwithstanding, each parameter had a specific impact on pollutant transport, which was not very prominently observed among these factors.

When water flows 1000m, the contaminant flows in the case of pH, IS, and HA; 500m, 500m, and 400 m respectively. This shows that clay layer was an important retarder for pollutant upward transport. This result was similar with findings of Liu Hui et al., (2013). The volumetric water content (θ) of the clay layer column in our experiment was much lower. Between the sorbent particles, a large amount of small-size micropores may have been formed, which, together with the inner micropores particles, tends to be type-2 sites. From the simulation, it's clear that this experiment tends to be more non-equilibrium, type2.

Table 4 Retardation coefficient

Parameters	R	1/R	β
pH5	1.95	0.5	2.38
pH7	2.22	0.4	2.97
pH10	1.67	0.59	0.33
pH + AS	1.33	0.75	0.27
Is[0.001]	2.01	0.5	0.34
IS[0.01]	1.91	0.5	0.33
IS[0.1]	2.35	0.4	0.23
IS+AS	2.35	0.4	0.25
HA	2.35	0.4	0.5
HA+AS	1.67	0.59	0.24

5. CONCLUSIONS AND RECOMMENDATION

The purpose of this research was to study the co-transport of arsenate in the presence of iron hydroxide. Effects of pH, HA, and ionic strength (IS) on arsenate during the co-transport were also studied. In acidic conditions, the $Fe(OH)_3$ precipitates and the co-transport did not occur. This was the same in strong basidic condition. The most efficient pH value was found in the range 7 to 8, a condition that facilitates the co-transport of Fe $(OH)_3$ with arsenate.

In the presence of ionic strength, increase in salt concentration resulted in an increase in adsorption and decreased the transportation. In the presence of HA, the nanoparticles demonstrated high affinity for HA and the mobility became lesser and this prevented arsenate from adsorbing on to the nanoparticles surface, which consequently increased its mobility. HA plays important role in reducing the adsorption of arsenate. Here the colloid became less effective to bind the contaminant, preferentially allowing for more HA binding site.

Furthermore, we observed in this experiment that nanoparticles transport was influenced by the following; ionic strength, ionic composition, flow velocity, nature and size of suspended nanoparticles. The most significant of these factors under the conditions investigated in these column experiments were pH, ionic composition and particle size. From the 1/R value calculated, it reveals that when water flows a certain distance, the pollutant transport was half of the flow distance. The pH, ionic strength and the humic acid had an impact on the fate of arsenic transport.

Future research should focus on the retention particles (RPs) during the co-transport of iron hydroxide with arsenate in saturated conditions.

Acknowledgements

This work was financially supported by the National high technology research and development program "Natural groundwater remediation and demonstration" 2012 AA062602 and the Chinese Scholarship Council (CSC). We thank Mr. Liao Pang for his technical support. Special thanks to Mr. Zakari Sissou who helped with the data simulation.

REFERENCES

[1] Andreas Kappler, Marcus Benz, Bernhard Schink, Andreas Brune: Electron shuttling via humic acids in microbial iron (III) reduction in a freshwater sediment Fachbereich Biologie, Lehrstuhl fu«r Mikrobielle Oº kologie und Limnologie, Universita«t Konstanz, Fach M

654, 78457 Konstanz, Germany. FEMS, Microbiology Ecology, 2004, 47, 85-92.

[2] Ben-Moshe, T., Dror, I., Berkowitz, B.: Transport of metal oxide nanoparticles in saturated porous media. Chemosphere, 2010, 81 (3), 387-393.

[3] Cameron D.A and A. Klute: Convective-dispersive solute transport with a combined equilibrium and kinetic adsorption model.Water ressour.Res, 1977, 13:183-188.

[4] Dengjun Wang; Zhang Wei; Hao Xiuzhen; Zhou, Dongmei: Transport of Biochar Particles in Saturated Granular Media: Effects of Pyrolysis Temperature and Particle Size. Environ. Sci. Technol., 2013, 47 2, 821-828.

[5] Elimelech, M.: Effect of particle size on the kinetics of particle deposition under attractive double layer interactions. J. Colloid Interface Sci., 1994, 164, 190-199.

[6] Fuller, C. C., and Davis J.A.: Evaluation of the processes controlling dissolved arsenic in whitewood creek, South Dakota. U.S. Geological survey professional paper, 2003, 1681, 27-45.

[7] Hassellöv, M., Kammer F.v.d.: Iron oxide as geochemical nanovectors for metal transport in soileriver systems. Elements, 2008, 4, 399-404.

[8] Helland, A., Kastenholz, H., Thidell, A., Arnfalk, P., Deppert, K.: Nanoparticulate materials and regulatory policy in Europe: an analysis of stakeholder perspectives. J. Nanopart, 2006, 8, 709-719.

[9] Hofmann Thilo, Wendelborn Anke: Colloid facilitated transport of polychlorinated dibenzo-p-dioxins and dibenzofurans (PCDD/Fs) to the groundwater at Ma Da Area, Vietnam.Environmental Science and Pollution Research - InternationalVietnam. Environmental, 2007, 14 (4), 223-224.

[10] Ivan Carabante: Arsenic (V) Adsorption on Iron oxide. Implications for soil Remediation and water purofocation. Doctoral thesis. Lulea University of Technology, 2012, 5-13

[11] Lecoanet, H. F., Bottero, J., Wiesner, M. R.: Laboratory assessment of the mobility of anomaterials in porous media. Environ. Sci. Technol., 2004, 38 (19), 5164-5169.

[12] Li, Y. S.; Wang, Y. G.; Pennell, K. D.; Abriola, L. M.: Investigation of the transport and deposition of fullerene (C60) nanoparticles in quartz sands under varying flow conditions. Environ. Sci. Technol. 2008, 42 (19), 7174−7180.

[13] Liping Pang, Murray Close, Daniela Schneider, Greg Stanton: Effect of pore-water velocity on chemical nonequilibrium transport of Cd, Zn, and Pb in alluvial gravel columns. Institute of Environmental Science & Research Ltd., P.O. Box 29181, Christchurch, New Zealand , Journal of contaminant and hydrology, 2002, 57(3-4), 241–258.

[14] Lui Hui, Dan Zhang, Minjing Li, Lei Tong, Liang Feng: Competitive adsorption and transport of phthalate esters in the clay layer of JiangHan plain, State Key Laboratory of Biogeology and Environmental Geology, School of Environmental Studies, China University of Geosciences, Wuhan 430074, PR China, Chemosphere, 2001, 92(11), 2013, 1542–1549,

[15] Megan Seymour: Transport of Engineered Nanomaterials in Porous Media: Groundwater Remediation Application and Effects of Particle Shape. University of Nebraska-Lincoln, Lincoln, Nebraska, november, 2012,1-111.

[16] Michael F. Hochella Jr.,1 Steven K. Lower,2 Patricia A. Maurice,3 R. Lee Penn,4 Nita Sahai,5 Donald L. Sparks,6 Benjamin S. Twining: Nanominerals, Mineral Nanoparticles, and Earth Systems. Science, 2008; ,319, 1631-1635

[17] Mueller N.C., Nowack B.: Exposure modeling of engineered nanoparticles in the environment. Environmental Science & Technology, 2008, 42 , 4447–4453.

[18] Munjed A. Maraqa,, Xianda Zhao, Jae-ug Lee, Fathi Allan, Thomas C. Voice: Comparison of non-ideal sorption formulations in modeling the transport of phthalate esters through packed soil columns. a Department of Civil and Environmental Engineering,

United Arab Emirates University, P.O. Box 17555, Al Ain, United Arab Emirates. CTI and Associates, Inc., 51331 W. Pontiac Trail, Wixom, MI, USA. Department of Mathematical Science, United Arab Emirates University, Al Ain, United Arab Emirates. Department of Civil and Environmental Engineering, Michigan State University, East Lansing, MI 48824, USA. Journal of Contaminant Hydrology, 2011, 125 , 57–69.

[19] Puls, R.W., and Powell, R.M.: Transport of inorganic colloids through natural aquifer material: Implication for contaminants transport. Environ. Sci. Technol., 1992, 26, 614-621.

[20] Roco, M.C.: Environmentally responsible development of nanotechnology. Environ. Sci. Technol., 2005, 39, 106-112.

[21] Selim H.M., Davidson J.M., and R.S. Mansell.: Evaluation of two site adsorption model for describing solute transport in the soils. In proc. Summer computer simulation conf., Washington, D. C.,1976, 444-448;

[22] Siegrist, M., Wiek, A., Helland, A., Kastenholz, H.: Risks and nanotechnology: the public is more concerned than experts and industry. Nat. Nanotechnol, 2007, 2, 67.

[23] Simunek, J., van Genuchten, M.T., Sejna, M.: Development and applications of the HYDRUS and STANMOD software packages and related codes. Vadose Zone J. , 2008,7, 587–600.

[24] Smedley P.L., Kinniburgh D.G.: A review of the source, behaviour and distribution of arsenic in natural waters .British Geological Survey, Wallingford, Oxon OX10 8BB, K., Applied Geochemistry, 2001, 17 (5), ,517-568.

[25] Tiziana Tosco, Julian Bosch, Rainer U. Meckenstock, and Rajandrea Sethi: Transport of Ferrihydrite Nanoparticles in Saturated Porous Media:Role of Ionic Strength and Flow Rate: By Dipartimento di Ingegneria dell'Ambiente, del Territorio e delle Infrastrutture, Politecnico di Torino, corso Duca degli Abruzzi 24,10129 Torino, Italy ‡Helmholtz Zentrum München German Research Center for Environmental Health, Institute of Groundwater Ecology,Ingolstädter Landstr. 1, D-85764 Neuherberg, Germany, Environ. Sc. Technol., 2012, 46, 4005-4015

[26] Tufenkji, N., Elimelech, M.: Correlation equation for predicting single-collector efficiency in physicochemical filtration in saturated porous media. Enviro. Sci.Technol., 2004, 38 (2), 529-536.

[27] Vangenuchten, M.T., Wagenet, R.J.:2-Site 2-region models for pesticide transport and degradation – theoretical development and analytical solutions. Soil Sci. Soc. Am. J.,1989, 53, 1303–1310.

[28] Wang, C., Bobba, A. D., Attinti, R., Shen, C., Lazouskaya, V., Wang, L., Jin, Y., Retention and transport of silica nanoparticles in saturated porous media: effect of concentration and particle size. Environ. Sci. Technol., 2012, 46 (13), 7151-7158.

[29] Wei, Xiaorong, Shao, Mingan, Horton, Robert, Han and Xinning: Humic Acid Transport in Water-Saturated Porous Media. Envionmental modeling assessment, 2010, 15, (11), 55-63.

[30] Waychunas, G.A., Rea B.A., Fuller C.C., and Davis J.A.: Surface chemistry of ferrihydrite: Part 1. EXAFS studies of the geometry of coprecipitated and adsorbed arsenate. Geochim. Cosmochim, 1993, 57, 2251–2269.

[31] Yao, K., Habibian, M. T., O'Melia, C. R.: Water and wastewater filtration: concepts and applications. Environ. Sci. Technol., 1971, 5 (11), 1105-1112.

[32] Yang X., Flynn R., von der Kammer F., Hofmann T.: Quantifying the influence of humic acid adsorption on colloidal microsphere deposition onto iron-oxide-coated sand. School of Planning, Architecture & Civil Engineering, Queen's University Belfast, David Keir Building, Stranmillis Road, Belfast, BT9 5AG Northern Ireland, UK. Department of Environmental Geosciences, University of Vienna, Althanstrasse, Environmental pollution, 2010, 14, 3496-3506.

[33] Zhang Hua and Selim: Modeling the Transport and Retention of Arsenic (V) in Soils.Sturgis Hall, Dep. of Agronomy and Environmental Management, Louisiana State Univ. Agric. Center, Baton Rouge, LA 70803-2110 and H. M. Selim, Department of Agronomy and Environmental Management, LSU Agcenter, Louisiana State University, Baton Rouge. Contaminant hydrology, 2006,126 (3-4), 121-126.

